Testing and Simulating the Response of a New Tracking Sensor for the ATLAS Detector

Ryan Justin Atkin

Department of Physics, University of Cape Town, Private Bag X3, Rondebosch 7701, Cape Town, South Africa

E-mail: rjatkin93@gmail.com

Abstract. The Large Hadron Collider (LHC) will undergo upgrades to the High Luminosity LHC (HL-LHC) in 2024, increasing the instantaneous luminosity almost four fold. This will require the detectors to be upgraded in order to cope with the large increase in data rates and radiation as well as improving the tracking and particle reconstruction in the higher occupancy environment. A major upgrade to the ATLAS detector will be replacing the current Inner Detector (ID) with a fully silicon semiconductor-based Inner Tracker (ITk). The sensors in the ITk strip forward region will use radial geometries, however until now the testbeam simulation and reconstruction software packages were designed with cartesian geometries. Presented is the work behind implementing a radial geometry and co-ordinate system, as well as a charge propagation model for one of the ITk strip forward sensors, the R0 module, in these testbeam software packages. The data from the EUDET testbeam telescope at DESY, Hamburg, and the simulated data both undergo the same reconstruction. A comparison between the two is performed in order to validate the radial geometry and charge propagation model.

1. Introduction

With new physics searches pushing the limits of the current Large Hadron Collider (LHC) [1] and its detectors, an upgrade of the LHC to the High Luminosity LHC (HL-LHC) [2] has been planned. The principal upgrade will occur during the third Long Shutdown (LS3) starting at the beginning of 2024 [3]. The upgrade will increase the instantaneous luminosity to an ultimate value of $\mathscr{L}_{ins} = 75\text{nb}^{-1}.\text{s}^{-1}$ [3], around 7.5 times the design luminosity. This will result in a total integrated luminosity of around $\mathscr{L} = 4000\text{fb}^{-1}$ during the 10 years of operation and up to an average of $\mu = 200$ collisions per bunch crossing. These improvements will greatly increase the statistics available for analysis while at the same time exceeding the current detectors' design capabilities with respect to pile-up management and radiation tolerance. Therefore the detectors will require an upgrade themselves. In particular, the ATLAS detector's main upgrades (phase-2 upgrades) will occur during LS3 (2024-2026) as laid out in the Letter of Intent (LoI) [4]. The focus will be on upgrading the current Inner tracking Detector (ID) to the full silicon semiconductor Inner Tracker (ITk) [3]. The purpose of the ID upgrade is to improve the tracking resolution as well as cope with the higher occupancy environment and radiation doses.

1.1. ITk

The current ID was designed to deal with an average of 23 proton-proton collisions per bunch crossing, not the proposed 200 during the HL-LHC phase [3]. The current resolution of the

Table 1. The specifications of the R0 module [5]. Rows 0 and 1 were read out by one hybrid, while rows 2 and 3 were read out by another hybrid. The pitch is the distance from the centre of a strip to the centre of the next strip.

Row number	nChips	nStrips	Inner Radius [mm]	Length [mm]	Angular Pitch [μrad]	Min/Max pitch [μm]
0	8	1026	384.500	18.981	193.3	74.3/78
1	8	1026	403.481	23.981	193.3	78/82.6
2	9	1154	427.462	28.980	171.8	73.5/78.4
3	9	1154	456.442	31.981	171.8	78.4/83.9

ID would make pattern recognition difficult and provide a poor track finding efficiency in the higher occupancy environment. The ITk will be a full silicon semiconductor tracker with forward (endcap, $|\eta| > 1.8$) and central (barrel, $|\eta| < 1.8$) regions divided into the strip detector (elongated read-outs capable of measuring 1 spatial co-ordinate) and the pixel detector (square read-outs capable of measuring 2 spatial co-ordinates). The tracking pseudorapidity range will be increased to $|\eta| < 4$, which will be important for electro-weak and new physics searches, as well as improving missing transverse momentum resolution and pile-up jet rejection [3].

2. R0 module

The R0 module is located in the ITk strip endcap, and is the closest module in that region to the interaction region [3]. A module is a composite device composed of a power board and one or two hybrids (kapton board with read-out chips) glued to a silicon semiconductor sensor. An image of the R0 module showing the sensor and hybrids is given in Fig. 2. The shape of the R0 sensor is known as a stereo annulus; it has the inner and outer curved edges concentric to the interaction region while the straight sides converge to a point offset in (x, y) from the interaction point. The strips are placed parallel to the straight sides and focus on the same offset point, providing the strips an angle of 20 mrad off the radial line (stereo angle) [3]. As the strips are only capable of measuring 1 spatial co-ordinate, the combination of strip sensors on either side of a petal with the stereo angle allows for the measurement of the second spatial co-ordinate. The R0 module has two hybrids each reading out two rows of strips. The two inner rows will have a different angular pitch to the two outer rows [5], where the pitch is the distance from the center of one strip to the next. Some of the R0 specifics are given in Table 1. The readout chips provide a 1-bit digital output that only stores a yes or no if the charge collected in a strip is over a predefined threshold charge.

3. Testbeam

The testbeam telescope is a EUDET-type telescope [6] operated by the EUDAQ framework and is located at DESY in Hamburg, Germany. A carbon fibre target in the DESY II e^+/e^- accelerator produces bremsstrahlung radiation that passes through a metal plate converter, producing more e^+/e^- pairs [6]. These electrons pass through a dipole magnet which selects 4.4 GeV electrons to be used as the test beam. The telescope comprises of six Mimosa26 high granularity pixel detectors [7], as shown in Fig. 2, that are used for track finding. The sensor that is being tested is known as a Device Under Test (DUT) and is placed between the third and fourth mimosa detectors. An additional FE-I4 sensor is used to improve the timing of the triggers.

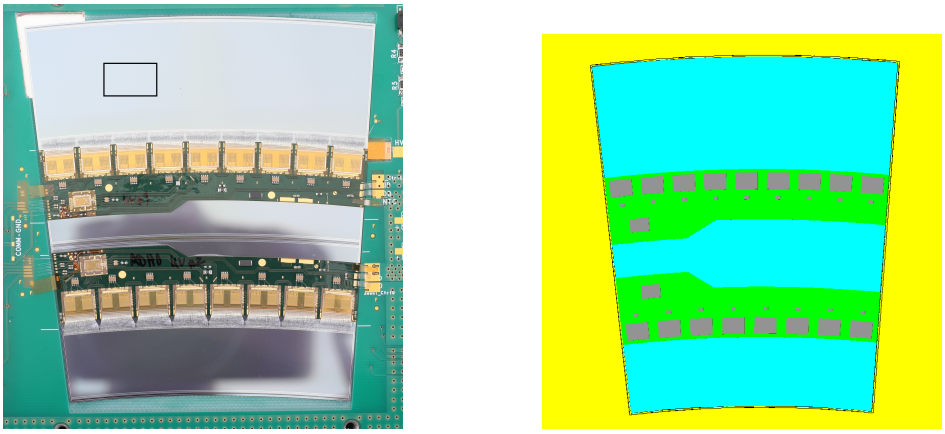

(a) (b)

Figure 1. An image of the R0 module tested in the testbeam (a) and the simulation of that module (b). The green boards going across the sensor are the hybrids, with the readout chips and hybrid controller chip. The black square in (a) is roughly the position and size of the beam for this study.

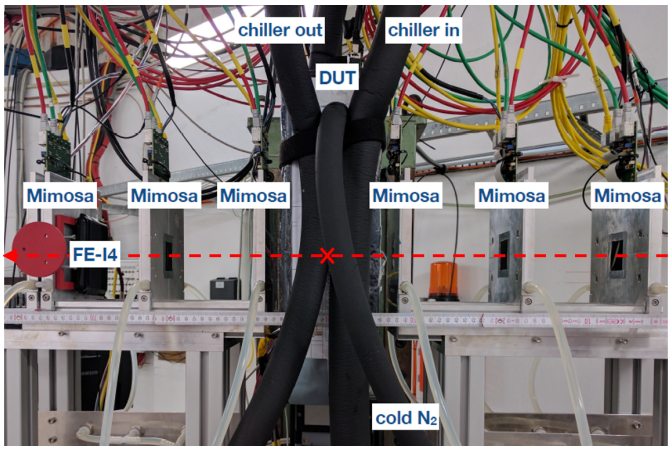

Figure 2. Image of the EUDET testbeam telescope at DESY. Shown are the six mimosa pixel detectors used for beam tracking, the Device Under Test (DUT) and the FE-I4 timing detector. The beam follows the red dashed line from right to left, and the interaction with the DUT occurs at the cross.

4. Simulation, Reconstruction and Analysis

The simulation of the R0 sensor in the testbeam telescope was performed using AllPix [8], a Geant4 [9] based simulator dedicated to the study of solid state detectors. AllPix was developed as a generic simulator for pixel detectors, although it has an important application in the simulation of EUDET-type testbeam telescopes due to the pre-defined detectors and telescope setups. AllPix not only defines the geometries of the sensors, but also simulates the response of the readout chips to the deposited charge for each specific detector. Strips with a deposited charge above a threshold are readout as hits. The reconstruction is performed using EUTelescope [10], a generic pixel-telescope data analysis framework. The software is used to reconstruct the tracks from both the testbeam telescope as well as the AllPix simulation data. Adjacent hits

on each sensor are clustered, and only the clusters across all six mimosa planes are fit to create proto-tracks, which are then used to align all the sensors. After alignment, a final fit of the mimosa clusters is performed to create the final tracks. The final tracks are extrapolated to find the (x, y) position of that track on the DUT. A cluster on the DUT is matched to the track if it lies within a particular distance from the track. The output of the reconstruction is the cluster and track positions in each sensors' local reference frame. This output underwent further analysis to calculate the phi residuals, interstrip clustering and interstrip efficiencies. The phi residual is the distance between the clusters' and reconstructed tracks' phi co-ordinates. The interstrip clustering shows how the probability of a cluster size being greater than 1 changes as we move from one side of a strip to the other. In other words, the probability that the deposited charge in the sensor is shared between neighbouring strips and is over threshold in those strips.

5. Results

This study looked at 4 different thresholds at a position in the fourth row of strips on the R0 sensor, shown in Fig. 1(a). A summary of the phi residuals and charge sharing for the different thresholds is given in Table 2. The uncertainties are purely statistical and are calculated assuming Poisson distributions. The systematic uncertainties from the charge propagation model were not taken into account. Before comparing the effects of different thresholds, a comparison between experiment and simulation is discussed at the threshold of 0.75 fC. The interstrip sharing, shown in Fig. 3(b), matches well between experiment and simulation, however the simulation is slightly higher near the strip edges and lower at the points of curvature around ± 0.3 from the centre of the strip. This is most likely due to the simulation having no noise or random effects added in the propagation of the charges. The interstrip sharing also shows how the probability of sharing in the central region of the strip is consistently very low and that it increases as the incident particle gets closer to the edge. The phi residual is given in Fig. 3(a). The experiment and simulation match very well, and both have a clear secondary peak from clusters of size greater than one due to the lower threshold of this run. The expected phi resolution for the strips in this row, based on single strip clusters, is ~ 49 μrad. The standard deviation of both simulation and experiment residuals are slightly lower than this, as seen in Table 2, since the threshold is low and sharing is relatively high. The plots comparing the different thresholds for the residuals and interstrip clustering are given in Fig. 4 and 5 respectively. As the threshold increases, the secondary peak in the residuals for experiment and simulation gets smaller and eventually disappears. The 3.05 fC threshold samples have almost all clusters as 1 strip clusters, and so have residual resolutions very close to the expected value of ~ 49 μrad. The experimental residual has started to round off at the centre for the 3.05 fC threshold data, becoming more gaussian, while the simulation has flat topped. This is most likely due to some of the electrons in the experiment depositing charge lower than the threshold which does not occur in the simulation since noise is not simulated. The peaks in the sharing plots also drop as the threshold increases, since the threshold becomes larger than the amount of charge shared between the strips. The difference in the values for sharing between experiment and simulation could be due to the one dimensional electric field modeling and no use of noise or random gaussian spreads in the threshold. The conversion of the threshold into femtocoulombs was an approximate fit and so may not be very accurate as well.

6. Conclusion

Due to the HL-LHC upgrade, the ATLAS detector will require an upgrade to cope with the new high pile-up environment. Part of the R&D for this upgrade was the testing and simulation of one of the ITk forward strip modules in a testbeam telescope.

The simulation of the testbeam telescope was compared to the results from the actual experiment. The experimental data performs as was expected for the R0 sensor based on

Table 2. Summary of the experimental (Exp) and simulation (Sim) results for the different thresholds. Shown is the resolution from the residuals, the probability of sharing, and the efficiency. All uncertainties are statistical.

Threshold [fC]	Residual [μrad]		Sharing [%]	
	Exp	Sim	Exp	Sim
0.75	48.78 ± 0.13	47.89 ± 0.07	12.80 ± 0.18	12.48 ± 0.08
1.62	51.19 ± 0.13	51.18 ± 0.08	4.92 ± 0.1	5.66 ± 0.05
2.33	49.90 ± 0.14	51.3 ± 0.08	2.78 ± 0.08	2.98 ± 0.04
3.05	48.66 ± 0.20	49.43 ± 0.08	2.31 ± 0.1	2.10 ± 0.03

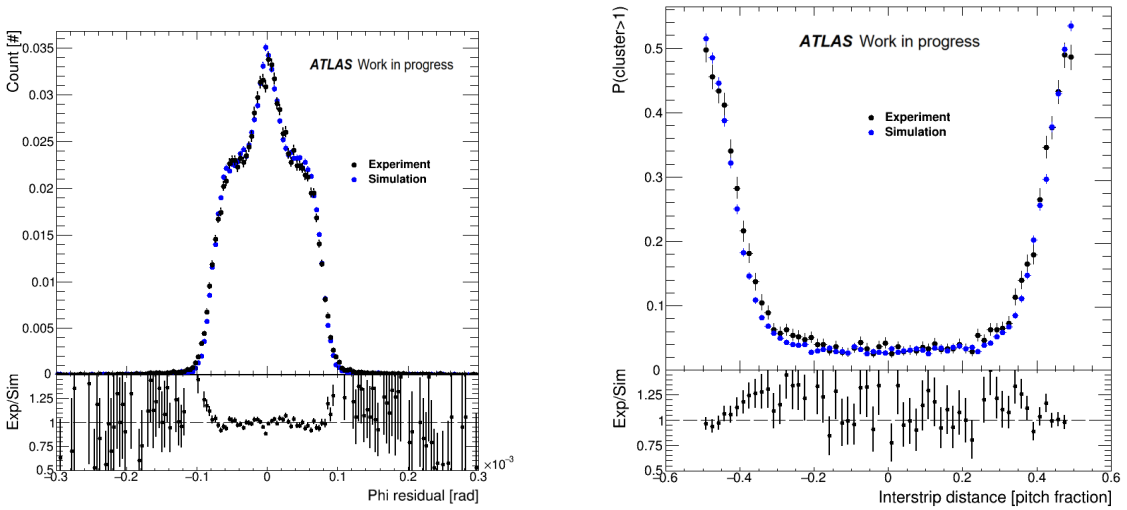

(a) (b)

Figure 3. The interstrip clustering (a) and phi residuals normalised to one (b) for the 0.75 fC run. The black points represent the experimental data while the blue points represent the simulated data. The secondary peaks in (b) are due to clusters of size 2.

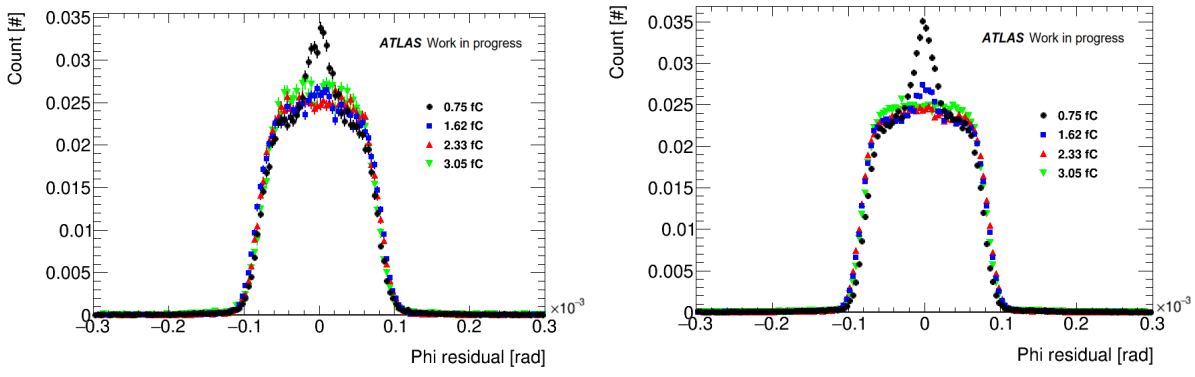

(a) (b)

Figure 4. The phi residuals normalised to one for the experiment (a) and simulation (b) at four different thresholds. The secondary peaks at the lower thresholds are due to clusters of size 2.

 ISBN: 978-0-620-88875-2

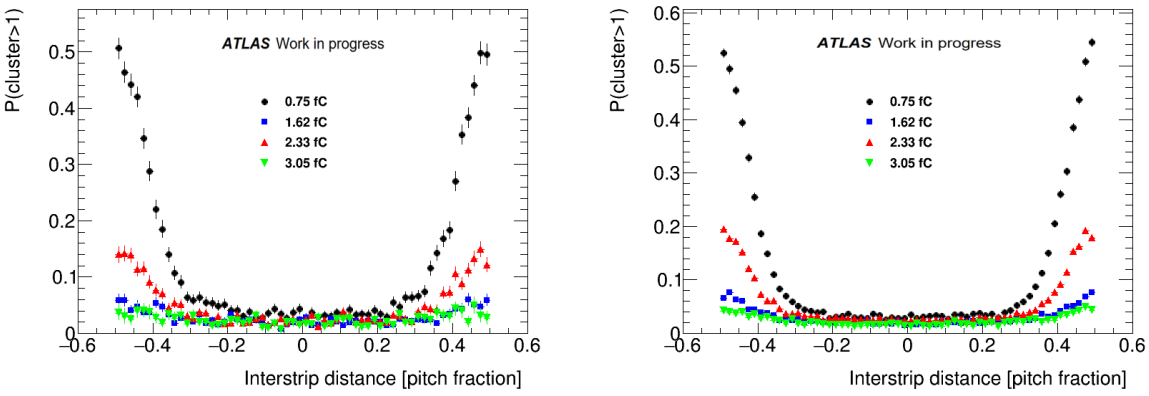

Figure 5. The interstrip clustering for the experiment (a) and simulation (b) at four different thresholds. Interstrip clustering is the probability of a cluster having a size greater than one as a function of the position of a track within a strip.

previous tests done on other strip sensors. This indicates that the radial geometry definitions in EUTelescope provides very good reconstruction of radial data, and that the sensors can go into full production. The simulation of the R0 sensor in terms of both the geometry and the charge propagation works well, predicting how the actual R0 sensor would behave in the testbeam telescope. Improvements to these results would be the inclusion of electronic noise during the digitisation stage of the R0 simulation, more accurately simulating the non-silicon material in the testbeam telescope and having a more accurate threshold conversion.

Acknowledgments

I would like to thank my supervisor Dr. Sahal Yacoob as well as my co-supervisors Dr. Kenneth G. Wraight, Dr. Stephen W. Peterson and Dr. Andrew Blue for their important input and assistance, the NRF for funding my MSc studies and as part of the AIDA2020 project: This project has received funding from the European Unions Horizon 2020 Research and Innovation programme under Grant Agreement no. 654168.

References

[1] Lyndon Evans and Philip Bryant. LHC Machine. *Journal of Instrumentation*, **3**(08):S08001, 2008.
[2] I Bejar Alonso and L Rossi. HiLumi LHC Technical Design Report: Deliverable: D1.10. Technical Report CERN-ACC-2015-0140, Nov 2015.
[3] ATLAS Collaboration. Technical Design Report for the ATLAS Inner Tracker Strip Detector. Technical Report CERN-LHCC-2017-005. ATLAS-TDR-025, CERN, Geneva, Apr 2017.
[4] ATLAS Collaboration. Letter of Intent for the Phase-II Upgrade of the ATLAS Experiment. Technical Report CERN-LHCC-2012-022. LHCC-I-023, CERN, Geneva, Dec 2012.
[5] ATLAS Upgrade Strip Sensor Collaboration. Supply of Silicon Microstrip Sensors of ATLAS12EC specifications. Technical report, 2016.
[6] Hendrik et al. Jansen. Performance of the eudet-type beam telescopes. *EPJ Techniques and Instrumentation*, 3(1):7, 2016.
[7] M. Winter. Development of Swift, High Resolution, Pixel Sensor Systems for a High Precision Vertex Detector suited to the ILC Running Conditions. Technical Report DESY PRC R&D Nr 01/04, 2009.
[8] M. Benoit and J. Idarraga. The AllPix Simulation Framework, 2014.
[9] Geant4 Collaboration. GEANT4: A Simulation toolkit. *Nucl. Instrum. Meth.*, A506:250–303, 2003.
[10] A. Bulgheroni, T. Klimkovich, P. Roloff, and A.F. Zarnecki. EUTelescope: tracking software. Technical Report EUDET Memo-2007-20, 2007.